Experimental review of τ lepton studies at the B factories

Denis Epifanov[1,2,*]

[1] *Novosibirsk State University, Novosibirsk 630090*
[2] *Budker Institute of Nuclear Physics SB RAS, Novosibirsk 630090*

Abstract. Recent results of a high-statistics τ lepton studies at B factories are reported. Reviewed are the measurements of Michel parameters in leptonic and radiative leptonic τ decays at Belle, as well as the measurement of the branching fractions of the radiative leptonic τ decays at *BABAR*. Searches for CP symmetry violation in hadronic decays with K_S^0 are also briefly discussed.

1 Introduction

The world largest data set of τ leptons collected at e^+e^- B factories [1] opens new era in the precision tests of the Standard Model (SM). An essential progress has been made in the study of the main τ properties at Belle and *BABAR*, namely, lifetime [2, 3], mass [4, 5], EDM [6] have been measured with the best or competitive to the world best accuracies.

In the SM, τ decays due to the charged weak interaction described by the exchange of $W^\pm$ with a pure vector coupling to only left-handed chirality fermions. There are two main classes of tau decays: leptonic decays[1] ($\tau^- \to \ell^- \bar{\nu}_\ell \nu_\tau$, $\tau^- \to \ell^- \bar{\nu}_\ell \nu_\tau \gamma$, $\tau^- \to \ell^- \ell'^+ \ell'^- \bar{\nu}_\ell \nu_\tau$; $\ell, \ell' = e, \mu$), and hadronic decays. Leptonic decays are the only ones in which the electroweak couplings can be probed without disturbance from the strong interactions. This makes them an ideal system to study the Lorentz structure of the charged weak current. Recently, leptonic and radiative leptonic τ decays have been studied at B factories. While Belle focused on the measurement of Michel parameters in these decays [7, 8], *BABAR* performed precision tests of the lepton universality [9] and measurement of the branching fractions [10].

Hadronic decays of τ offer unique tools for the precision studies of low energy QCD [11]. Of particular interest are strangeness changing Cabibbo-suppressed hadronic τ decays, in which large CP symmetry violation (CPV) could appear from a charged scalar boson exchange [12].

2 Measurement of Michel parameters in τ decays at Belle

2.1 Ordinary leptonic τ decays

In the low-energy four-fermion framework, the matrix element of leptonic τ decay can be written in the generalized form with ten possible Lorentz structures, which are characterized by ten complex coupling constants g_{ij}^N, $i, j = L, R$; $N = S, V, T$ ($g_{RR}^T, g_{LL}^T \equiv 0$). Indices i and j label the

---

[*] e-mail: D.A.Epifanov@inp.nsk.su
[1] Unless specified otherwise, charge conjugate decays are implied throughout the paper.

left- and right-handedness of the charged leptons, index N denotes the properties of the currents under Lorentz transformation (scalar(S), vector(V), tensor(T)). In the SM, the only non-zero coupling constant is $g_{LL}^V = 1$, this property is also known as (V-A)⊗(V-A) Lorentz structure of the matrix element. In the case where neutrinos are not detected and the spin of the outgoing charged lepton is not determined, only four Michel parameters (MP) ρ, η, ξ and δ are experimentally accessible, they are bilinear combinations of the g_{ij}^N coupling constants [13, 14]. In the SM, the (V-A) charged weak current is characterized by $\rho = 3/4$, $\eta = 0$, $\xi = 1$ and $\delta = 3/4$.

While ρ and η parameters appear in the predicted energy spectrum of the charged lepton, spin-spin correlations between the τ^+ and τ^- produced in the reaction $e^+e^- \rightarrow \tau^+\tau^-$ are exploited to measure also ξ and δ MP [15]. Events where signal tau decays leptonically, $\tau^- \rightarrow \ell^-\bar{\nu}_\ell\nu_\tau$, while the opposite tau decays via $\tau^+ \rightarrow \pi^+\pi^0\bar{\nu}_\tau$ (it is characterized by ξ_ρ, in the SM $\xi_\rho = 1$) are selected for the analysis. The total differential cross section, $\frac{d\sigma}{d\vec{z}}(\vec{\Theta})$ ($\vec{\Theta} = \{1, \rho, \eta, \xi_\rho\xi, \xi_\rho\xi\delta\}$, $\vec{\Theta}_{SM} = \{1, 3/4, 0, 1, 3/4\}$), is used to construct the probability density function (p.d.f.) for the measurement vector $\vec{z} = \{p_\ell, \cos\theta_\ell, \phi_\ell, p_\rho, \cos\theta_\rho, \phi_\rho, m_{\pi\pi}, \cos\tilde{\theta}_\pi, \tilde{\phi}_\pi\}$. Michel parameters are extracted in the unbinned maximum likelihood fit of the ($\tau^- \rightarrow \ell^-\bar{\nu}_\ell\nu_\tau$; $\tau^+ \rightarrow \pi^+\pi^0\bar{\nu}_\tau$) ($\ell = e, \mu$) (or, briefly, ($\ell^-$; ρ^+)) events in the full nine-dimensional phase space [16, 17]. The main background processes, (ℓ^-; $\pi^+\pi^0\pi^0$), (π^-; ρ^+) and (ρ^-; ρ^+) with the fractions, $\lambda_{3\pi}$, λ_π and λ_ρ, respectively, are included in the p.d.f. analytically. The remaining background with the fraction λ_{other} is described by the $\mathcal{P}_{bg}^{MC}(\vec{z})$ p.d.f., which is evaluated from the large Monte Carlo (MC) sample [18]. The total p.d.f. is written as:

$$\mathcal{P}(\vec{z}) = \frac{\varepsilon(\vec{z})}{\bar{\varepsilon}}\Big((1 - \lambda_{3\pi} - \lambda_\pi - \lambda_\rho - \lambda_{other})\frac{S(\vec{z}|\vec{\Theta})}{\int \frac{\varepsilon(\vec{z})}{\bar{\varepsilon}}S(\vec{z}|\vec{\Theta})d\vec{z}}+$$

$$+\lambda_{3\pi}\frac{B_{3\pi}(\vec{z}|\vec{\Theta})}{\int \frac{\varepsilon(\vec{z})}{\bar{\varepsilon}}B_{3\pi}(\vec{z}|\vec{\Theta})d\vec{z}} + \lambda_\pi\frac{B_\pi(\vec{z})}{\int \frac{\varepsilon(\vec{z})}{\bar{\varepsilon}}B_\pi(\vec{z})d\vec{z}} + \lambda_\rho\frac{B_\rho(\vec{z})}{\int \frac{\varepsilon(\vec{z})}{\bar{\varepsilon}}B_\rho(\vec{z})d\vec{z}} + \lambda_{other}\mathcal{P}_{bg}^{MC}(\vec{z})\Big), \quad (1)$$

where $S(\vec{z}|\vec{\Theta})$, $B_{3\pi}(\vec{z}|\vec{\Theta})$, $B_\pi(\vec{z})$ and $B_\rho(\vec{z})$ are the cross sections for the (ℓ^-; ρ^+), (ℓ^-; $\pi^+\pi^0\pi^0$), (π^-; ρ^+) and (ρ^-; ρ^+) events, respectively; $\varepsilon(\vec{z})$ is the detection efficiency for signal events in the full phase space; and $\bar{\varepsilon} = \int \varepsilon(\vec{z})S(\vec{z}|\vec{\Theta}_{SM})d\vec{z}/ \int S(\vec{z}|\vec{\Theta}_{SM})d\vec{z}$ is an average signal detection efficiency.

The analysis is based on a 485 fb^{-1} data sample that contains 446×10^6 $\tau^+\tau^-$ pairs, collected at Belle [7]. After all selections, about 5.5 million events are selected for the fit. It is confirmed that the uncertainties arising from the physical and apparatus corrections to the p.d.f., as well as from the p.d.f. normalization are well below 1%, see Table 1. However, we still observe a systematic bias of

Table 1. Systematic uncertainties of MP. Values are shown in units of percent (i.e. absolute deviation of the MP is multiplied by 100%).

MP	Radiative corrections	Detector resolution	KEKB beam energy spread	Normalization of p.d.f.
$\sigma(\rho)$, %	0.10	0.10	0.07	0.21
$\sigma(\eta)$, %	0.30	0.33	0.25	0.60
$\sigma(\xi_\rho\xi)$, %	0.20	0.11	0.03	0.38
$\sigma(\xi_\rho\xi\delta)$, %	0.15	0.19	0.15	0.26

the order of a few percent, especially in the $\xi_\rho\xi$ and $\xi_\rho\xi\delta$ MP. This bias originates from the remaining inaccuracies in the description of the experimental trigger efficiency corrections.

2.2 Radiative leptonic τ decays

Emission of the photon in the final state of the radiative leptonic τ decay results in three additional Michel parameters: $\bar{\eta}$, η'' and $\xi\kappa$ [19]. Measurement of these parameters provides a further constraint on the Lorentz structure of the charged weak current. The $\xi\kappa$, like ξ and δ, appears in the τ spin-dependent part of the differential decay width, so, spin-spin correlations between the τ^+ and τ^- allow one to measure $\xi\kappa$. The total differential decay width of the radiative leptonic decay depends on seven Michel parameters: ρ, η, ξ, δ, $\bar{\eta}$, η'' and κ. In this analysis, ρ, η, ξ, δ and ξ_ρ parameters are fixed to their SM values. Also, feasibility study showed that the sensitivity to the η'' is very poor in comparison with the $\bar{\eta}$ and κ, so, η'' was also fixed to its SM expectation $\eta'' = 0$. In the signal events one tau decays to radiative leptonic mode, $\tau^- \to \ell^- \bar{\nu}_\ell \nu_\tau \gamma$, while the other tau decays via $\tau^+ \to \pi^+ \pi^0 \bar{\nu}_\tau$. The p.d.f. function for the vector of the measured parameters $\vec{z} = \{p_\ell, \cos\theta_\ell, \phi_\ell, p_\gamma, \cos\theta_\gamma, \phi_\gamma, p_\rho, \cos\theta_\rho, \phi_\rho, m_{\pi\pi}, \cos\tilde{\theta}_\pi, \tilde{\phi}_\pi\}$ is constructed from the total differential cross section of the reaction $e^+ e^- \to (\tau^- \to \ell^- \bar{\nu}_\ell \nu_\tau \gamma; \tau^+ \to \pi^+ \pi^0 \bar{\nu}_\tau)$ (or, shortly, $(\ell^- \gamma; \rho^+)$), $\frac{d\sigma}{d\vec{z}}(\vec{\Theta})$ ($\vec{\Theta} = \{1, \bar{\eta}, \xi\kappa\}$, $\vec{\Theta}_{SM} = \{1, 0, 0\}$), which is linear function of $\bar{\eta}$ and $\xi\kappa$. Michel parameters are extracted in the unbinned maximum likelihood fit of the $(\ell^- \gamma; \rho^+)$ events in the full twelve-dimensional phase space. The dominant background processes are ordinary leptonic decay with the photon from the external bremsstrahlung and radiative leptonic decay with the external bremsstrahlung for the $(e^- \gamma; \rho^+)$ events; ordinary leptonic decay plus beam background or initial/final state radiation photon for the $(\mu^- \gamma; \rho^+)$ events. The dominant background contributions are included in the p.d.f. analytically. The remaining background with the fraction λ_0 is described by the $\mathcal{P}^{MC}_{bg}(\vec{z})$ p.d.f., evaluated from the MC sample. The total p.d.f. reads:

$$\mathcal{P}(\vec{z}) = \left(1 - \sum_{i=0}^{2(5)} \lambda_i\right) \frac{S(\vec{z}\,|\,\vec{\Theta})\varepsilon(\vec{z})}{\int d\vec{z} S(\vec{z}\,|\,\vec{\Theta})\varepsilon(\vec{z})} + \sum_{i=1}^{2(5)} \left(\lambda_i \frac{B_i(\vec{z})\varepsilon(\vec{z})}{\int d\vec{z} B_i(\vec{z})\varepsilon(\vec{z})}\right) + \lambda_0 \mathcal{P}^{MC}_{bg}(\vec{z}),$$

where $S(\vec{z}\,|\,\vec{\Theta})$ is analytical cross section for the signal, $B_i(\vec{z})$ is analytical cross section of the ith background ($i = 1, 2$ for the $(e^- \gamma; \rho^+)$, and $i = 1 \div 5$ for the $(\mu^- \gamma; \rho^+)$ events), λ_i is the fraction of the ith background and $\varepsilon(\vec{z})$ is the detection efficiency in the full phase space.

The statistics of about 703 fb^{-1} collected at Belle, which contains 646×10^6 $\tau^+\tau^-$ pairs was used for the analysis [8]. Summary of the selected data sample is shown in Table 2. Figures 1(a) and 1(b) show the distribution of the photon energy and the spatial angle between lepton and photon for the $(\mu^- \gamma; \rho^+)$ sample. The $\bar{\eta}$ was measured to be $\bar{\eta} = -1.3 \pm 1.5 \pm 0.8$ only in the $(\mu^- \gamma; \rho^+)$ sample,

Table 2. Summary of event selection

Mode	$(e^- \gamma; \rho^+)$	$(e^+ \gamma; \rho^-)$	$(\mu^- \gamma; \rho^+)$	$(\mu^+ \gamma; \rho^-)$
N_{sel}	420005	412639	35984	36784
$\varepsilon^\dagger$ (%)	4.45 ± 0.19	4.43 ± 0.19	3.42 ± 0.15	3.39 ± 0.15
Purity (%)	28.9		56.5	

$\dagger$ The photon energy threshold in the τ-rest frame is 10 MeV.

because of the poor sensitivity to this parameter in the $(e^- \gamma; \rho^+)$ sample. The first error is statistical and the second one is systematic. The $\xi\kappa$ was measured to be $\xi\kappa = 0.5 \pm 0.4 \pm 0.2$ in both samples. Figure 1(c) shows result of the fit of the $(\mu^- \gamma; \rho^+)$ sample. Within the uncertainties $\bar{\eta}$ and $\xi\kappa$ are consistent with the SM expectations.
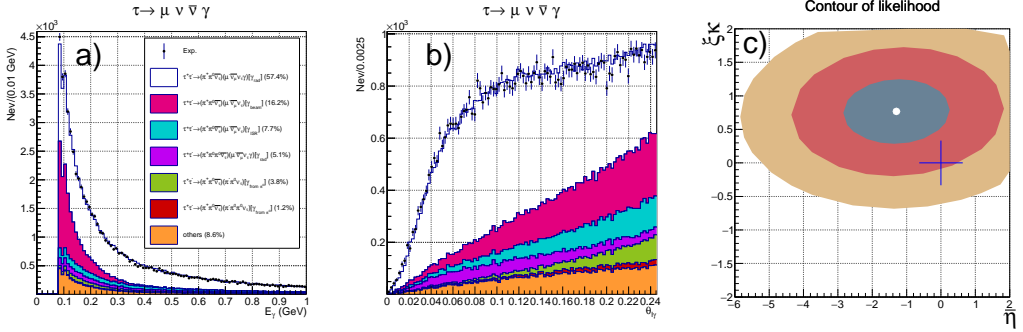
Figure 1. For the ($\mu^-\gamma$; ρ^+) sample: (a) photon energy E_γ, (b) spatial angle $\theta_{\mu\gamma}$ and (c) 1σ- 2σ- and 3σ-contours of the likelihood function on the $\bar{\eta} - \xi\kappa$ plane, the cross indicates SM prediction. Dots with error bars are experimental data and histograms are MC distributions.

3 Study of radiative leptonic τ decays at *BABAR*

The analysis is based on a 431 fb^{-1} data sample collected at *BABAR*, which corresponds to 400×10^6 τ-pairs [10]. Basically, events with track and photon from the signal tau and 1-prong decay of the second tau were selected.

Each of two oppositely charged tracks is required to have the transverse momentum $p_T > 0.3$ GeV/c, and the cosine of the polar angle $-0.75 < \cos\theta_{\text{track}} < 0.95$ to ensure good particle identification. The electron and muon identification efficiencies are 91% and 62%, respectively. The total missing transverse momentum of the event is required to be $p_{T,\text{miss}} > 0.5$ GeV/c. The photon energy threshold is 50 MeV. Each event is divided into two hemispheres (signal and tag hemispheres) in the center-of-mass (CM) frame by a plane perpendicular to the thrust axis. The magnitude of the thrust is required to be between 0.9 and 0.995. The signal hemisphere must contain one track and one photon. The tag hemisphere must contain one track, and possibly one additional photon or one or two π^0 candidates. Each π^0 candidate is reconstructed from a pair of photons with $\gamma\gamma$ invariant mass to be $100 \leq M_{\gamma\gamma} \leq 160$ MeV/c^2. The total energy deposition in the calorimeter is less than 9 GeV. In the signal hemisphere, the distance between the track and photon cluster, measured on the inner wall of the calorimeter, must be $d_{l\gamma} < 100$ cm. To suppress radiative $\mu^+\mu^-$ and Bhabha background, events with two leptons of the same flavors in the signal and tag hemispheres were rejected.

After these selections, both samples are dominated by background events. For the $\tau \to e\nu\bar{\nu}\gamma$ sample, the dominant background comes from the ordinary τ leptonic decay with the external bremsstrahlung in the material of the detector. For the $\tau \to \mu\nu\bar{\nu}\gamma$ sample, the main background comes from the initial-state radiation, $\tau \to \pi\pi^0\nu$ decays, $e^+e^- \to \mu^+\mu^-(\gamma)$ process, and $\tau \to \pi\nu$ decays.

Background was additionally suppressed applying cuts on the angle between lepton and photon in the CM frame ($\cos\theta_{l\gamma}$), invariant mass of the lepton-photon pair ($M_{l\gamma}$), photon energy in the CM frame (E_γ) and $d_{l\gamma}$. For the $\tau \to e\nu\bar{\nu}\gamma$ mode, the applied cuts are: $\cos\theta_{l\gamma} \geq 0.97$, $0.22 \leq E_\gamma \leq 2.0$ GeV (see Fig. 2(a)), $8 \leq d_{l\gamma} \leq 65$ cm, and $M_{l\gamma} \geq 0.14$ GeV/c^2. For the $\tau \to \mu\nu\bar{\nu}\gamma$, the applied selections are: $\cos\theta_{l\gamma} \geq 0.99$, $0.10 \leq E_\gamma \leq 2.5$ GeV (see Fig. 2(b)), $6 \leq d_{l\gamma} \leq 30$ cm, and $M_{l\gamma} \leq 0.25$ GeV/c^2. After applying all cuts the number of selected $\tau \to e\nu\bar{\nu}\gamma$ events is $N_{\text{sel}} = 18149 \pm 135$ with the fraction of background $f_{\text{bg}} = 0.156 \pm 0.003$; the number of selected $\tau \to \mu\nu\bar{\nu}\gamma$ events is $N_{\text{sel}} = 15688 \pm 125$ with the fraction of background $f_{\text{bg}} = 0.102 \pm 0.002$.
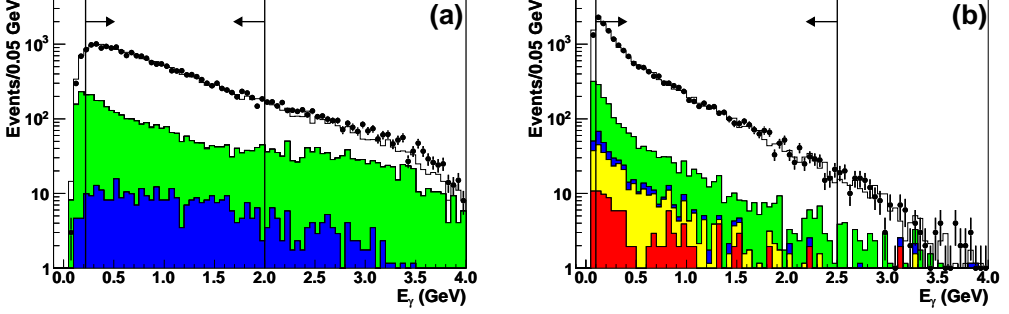
Figure 2. Photon energy in the CM frame: (a) for the $\tau \to e\nu\bar{\nu}\gamma$ mode, (b) for the $\tau \to \mu\nu\bar{\nu}\gamma$ mode.

The branching fraction is calculated as $\mathcal{B}_l = N_{\text{sel}}(1 - f_{\text{bg}})/(2\sigma_{\tau\tau}\mathcal{L}\epsilon_{\text{MC}})$, where $\sigma_{\tau\tau} = (0.919 \pm 0.003)$ nb is the cross section of the τ-pair production [20], $\mathcal{L} = 431$ fb^{-1} is the total integrated luminosity, and ϵ_{MC} is detection efficiency determined from the MC simulation. The efficiencies are $\epsilon_{\text{MC}} = (0.105 \pm 0.003)\%$ and $\epsilon_{\text{MC}} = (0.480 \pm 0.010)\%$ for the $\tau \to e\nu\bar{\nu}\gamma$ and $\tau \to \mu\nu\bar{\nu}\gamma$ modes, respectively. As a result: $\mathcal{B}(\tau \to e\nu\bar{\nu}\gamma) = (1.847 \pm 0.015 \pm 0.052) \times 10^{-2}$, $\mathcal{B}(\tau \to \mu\nu\bar{\nu}\gamma) = (3.69 \pm 0.03 \pm 0.10) \times 10^{-3}$, where the first error is statistical and the second one is systematic. The dominant contributions to the total systematic uncertainty come from the uncertainties on lepton identification and photon detection efficiency.

The measured branching ratios agree with the leading order (LO) SM predictions, $\mathcal{B}_{\text{LO}}(e\nu\bar{\nu}\gamma) = 1.834 \times 10^{-2}$, $\mathcal{B}_{\text{LO}}(\mu\nu\bar{\nu}\gamma) = 3.663 \times 10^{-3}$. However the next-to-leading order (NLO) SM prediction $\mathcal{B}_{\text{NLO}}(e\nu\bar{\nu}\gamma) = (1.645 \pm 0.019) \times 10^{-2}$ differs from *BABAR* experimental result by 3.5 standard deviations [21]. Hence, for the precision study of the radiative leptonic τ decay it is important to embed NLO corrections to the MC generator [22]. Also, the background from the doubly-radiative leptonic decays ($\tau \to l\nu\bar{\nu}\gamma\gamma$) should be properly studied.

4 CPV in τ decays with K_S^0

Recent studies of CPV in the $\tau^- \to \pi^- K_S^0(\geq \pi^0)\nu_\tau$ decays at *BABAR* [23] as well as in the $\tau^- \to K_S^0\pi^-\nu_\tau$ decay at Belle [24] provide complementary information about sources of CPV in these hadronic decays.

The decay-rate asymmetry $A_{\text{CP}} = \frac{\Gamma(\tau^+\to\pi^+ K_S^0(\geq\pi^0)\nu_\tau)-\Gamma(\tau^-\to\pi^- K_S^0(\geq\pi^0)\nu_\tau)}{\Gamma(\tau^+\to\pi^+ K_S^0(\geq\pi^0)\nu_\tau)+\Gamma(\tau^-\to\pi^- K_S^0(\geq\pi^0)\nu_\tau)}$ was studied at *BABAR* with a 476 fb^{-1} data sample. The obtained result $A_{\text{CP}} = (-0.36 \pm 0.23 \pm 0.11)\%$ is about 2.8 standard deviations from the SM expectation $A_{\text{CP}}^{K^0} = (+0.36 \pm 0.01)\%$.

At Belle, CPV search was performed as a blinded analysis based on a 699 fb^{-1} data sample. Specially constructed asymmetry, which is a difference between the mean values of $\cos\beta\cos\psi$ for τ^- and τ^+ events, was measured in bins of $K_S^0\pi^-$ mass squared ($Q^2 = M^2(K_S^0\pi)$):

$$A_i^{CP}(Q_i^2) = \frac{\int\limits_{\Delta Q_i^2} \cos\beta\cos\psi \left(\frac{d\Gamma_{\tau^-}}{d\omega} - \frac{d\Gamma_{\tau^+}}{d\omega}\right) d\omega}{\frac{1}{2}\int\limits_{\Delta Q_i^2} \left(\frac{d\Gamma_{\tau^-}}{d\omega} + \frac{d\Gamma_{\tau^+}}{d\omega}\right) d\omega} \simeq \langle\cos\beta\cos\psi\rangle_{\tau^-} - \langle\cos\beta\cos\psi\rangle_{\tau^+},$$

where β, θ and ψ are the angles, evaluated from the measured parameters of the final hadrons, $d\omega = dQ^2 d\cos\theta d\cos\beta$. In contrary to the decay-rate asymmetry, the introduced $A_i^{CP}(Q_i^2)$ is already sensitive to the CPV effects from the charged scalar boson exchange [12, 25]. No CP violation was observed and the upper limit on the CPV parameter η_S was extracted $|\mathrm{Im}(\eta_S)| < 0.026$ at 90% CL. Using this limit parameters of the Multi-Higgs-Doublet models [26, 27] can be constrained as $|\mathrm{Im}(XZ^*)| < 0.15\ M_{H^\pm}^2/(1\,\mathrm{GeV}^2/c^4)$, where $M_{H^\pm}$ is the mass of the lightest charged Higgs boson, the complex constants Z and X describe the coupling of the Higgs boson to leptons and quarks, respectively.

References

[1] A. J. Bevan *et al.* [BaBar and Belle Collaborations], Eur. Phys. J. C **74** (2014) 3026.

[2] K. Belous *et al.* [Belle Collaboration], Phys. Rev. Lett. **112** (2014) 031801.

[3] A. Lusiani [Babar Collaboration], Nucl. Phys. Proc. Suppl. **144** (2005) 105.

[4] K. Abe *et al.* [Belle Collaboration], Phys. Rev. Lett. **99** (2007) 011801.

[5] B. Aubert *et al.* [BaBar Collaboration], Phys. Rev. D **80** (2009) 092005.

[6] K. Inami *et al.* [Belle Collaboration], Phys. Lett. B **551** (2003) 16.

[7] D. A. Epifanov [Belle Collaboration], Nucl. Part. Phys. Proc. **287-288** (2017) 7.

[8] A. Abdesselam *et al.* [Belle Collaboration], Nucl. Part. Phys. Proc. **287-288** (2017) 11.

[9] B. Aubert *et al.* [BaBar Collaboration], Phys. Rev. Lett. **105** (2010) 051602.

[10] J. P. Lees *et al.* [BaBar Collaboration], Phys. Rev. D **91** (2015) 051103.

[11] A. Pich, Adv. Ser. Direct. High Energy Phys. **15** (1998) 453.

[12] S. Weinberg, Phys. Rev. Lett. **37** (1976) 657.

[13] W. Fetscher, H. J. Gerber and K. F. Johnson, Phys. Lett. B **173** (1986) 102.

[14] W. Fetscher and H. J. Gerber, Adv. Ser. Direct. High Energy Phys. **14** (1995) 657.

[15] Y. -S. Tsai, Phys. Rev. D **4** (1971) 2821 [Erratum-ibid. D **13** (1976) 771].

[16] W. Fetscher, Phys. Rev. D **42** (1990) 1544.

[17] K. Tamai, Nucl. Phys. B **668** (2003) 385.

[18] D. M. Schmidt, R. J. Morrison and M. S. Witherell, Nucl. Instrum. Meth. A **328** (1993) 547.

[19] A. B. Arbuzov and T. V. Kopylova, JHEP **1609** (2016) 109.

[20] S. Banerjee, B. Pietrzyk, J. M. Roney and Z. Was, Phys. Rev. D **77** (2008) 054012.

[21] M. Fael, L. Mercolli and M. Passera, JHEP **1507** (2015) 153.

[22] S. Jadach *et al.*, Comput. Phys. Commun. **76** (1993) 361.

[23] J. P. Lees *et al.* [BaBar Collaboration], Phys. Rev. D **85** (2012) 031102 [Erratum-ibid. D **85** (2012) 099904].

[24] M. Bischofberger *et al.* [Belle Collaboration], Phys. Rev. Lett. **107** (2011) 131801.

[25] J. H. Kuhn and E. Mirkes, Phys. Lett. B **398** (1997) 407.

[26] Y. Grossman, Nucl. Phys. B **426** (1994) 355.

[27] S. Y. Choi, K. Hagiwara and M. Tanabashi, Phys. Rev. D **52** (1995) 1614.